

1
2
3
4
5
6
7
8
9
10
11
12
13
14
15
16
17
18
19
20
21
22
23
24
25
26
27
28
29
30
31
32
33
34
35
36
37
38
39

Membrane stiffness is one of the key determinants of *E coli* MscS channel

mechanosensitivity

Feng Xue¹, Charles D. Cox^{1,2}, Navid Bavi³, Paul R Rohde¹, Yoshitaka Nakayama^{1,2} & Boris Martinac^{1,2*}*

¹Victor Chang Cardiac Research Institute
Lowy Packer Building
405 Liverpool St.
Darlinghurst, NSW 2010
Australia

²St Vincent's Clinical School
University of New South Wales
Darlinghurst, NSW 2010
Australia

³Institute for Biophysical Dynamics
University of Chicago
Chicago, USA.

*to whom correspondence should be addressed.
Email: b.martinac@victorchang.edu.au
Phone: +61 29295 8645
Email: y.nakayama@victorchang.edu.au
Phone: +61 29295 8645

Keywords: mechanosensation, mechanosensitive channels, electrophysiology, Patch fluorometry

40 **Abstract**

41 Prokaryotic mechanosensitive (MS) channels have an intimate relationship with
42 membrane lipids that underlie their mechanosensitivity. Membrane lipids may
43 influence channel activity by directly interacting with bacterial MS channels or by
44 influencing the global properties of the membrane such as elastic area expansion
45 modulus or bending rigidity. Previous work has implicated membrane stiffness as a
46 potential determinant of the mechanosensitivity of *E. coli* (*Ec*)MscS. Here we
47 systematically tested this hypothesis using patch fluorometry of azolectin liposomes
48 doped with lipids of increasing elastic area expansion modulus. Increasing
49 dioleoylphosphatidylethanolamine (DOPE) content of azolectin liposomes made it
50 more difficult to activate *Ec*MscS by membrane tension (i.e. increases its gating
51 threshold). This effect was exacerbated by the addition of stiffer forms of
52 phosphatidylethanolamine such as the branched chain lipid
53 diphytanoylphosphoethanolamine (DPhPE) and the fully saturated lipid distearoyl-sn-
54 glycerol-3-phosphoethanolamine (DSPE). Furthermore, a comparison of the branched
55 chain lipid diphytanoylphosphocholine (DPhPC) to the stiffer DPhPE indicated again
56 that it was harder to activate *Ec*MscS in the presence of the stiffer DPhPE. We show
57 that these effects are not due to changes in membrane bending rigidity as the membrane
58 tension threshold of *Ec*MscS in membranes doped with PC18:1 and PC18:3 remained
59 the same, despite a two-fold difference in their bending rigidity. We also show that after
60 prolonged pressure application sudden removal of force in softer membranes caused a
61 rebound reactivation of *Ec*MscS and we discuss the relevance of this phenomenon to
62 bacterial osmoregulation. Collectively, our data suggests that membrane stiffness
63 (elastic area expansion modulus) is one of the key determinants of the
64 mechanosensitivity of *Ec*MscS.

65
66
67
68
69
70
71
72
73
74
75
76
77
78
79
80
81
82
83

84 **Introduction**

85 The *E. coli* mechanosensitive (MS) ion channel of small conductance (*EcMscS*) is a
86 prototypical membrane tension sensor which plays a pivotal role in osmoregulation [1-
87 3]. This channel is the canonical member of a diverse family of MS channels that spans
88 prokaryotic and eukaryotic cell-walled organisms [4-6]. Purification and reconstitution
89 of *EcMscS*, and many of its homologues, into lipid bilayers show that it gates according
90 to the force-from-lipid principle [7-10]. This means the channel is inherently
91 mechanosensitive and directly senses membrane forces that result in a conformational
92 change culminating in the channel opening. As a result, it is clear that membrane lipids
93 are a key driver of *EcMscS* activity. Recent evidence suggests that eukaryotic MS
94 channels also employ force-from-lipids gating [11-14]. Therefore, the basic biophysical
95 principles that govern the gating of prokaryotic channels may in turn provide insight
96 into the gating of eukaryotic MS channels [15-17].

97
98 Liposomal reconstitution has been successfully used for many years not only to
99 document the inherent mechanosensitivity of both prokaryotic and eukaryotic ion
100 channels but also to probe the influence of individual lipids on channel function in
101 general [18-21]. Lipids can influence integral membrane proteins such as MS channels
102 in one of two ways [22]. Firstly, the lipid may “specifically” interact with the protein
103 and modify its function, acting as a ligand. The second is that lipids may influence
104 channel function via their global effects on the mechanical properties of the bilayer.
105 Two key bulk properties of the membrane in which the protein sits are the elastic area
106 expansion modulus and bending modulus. Both moduli are in fact the resultants of the
107 lateral pressure profile [23] and geometric properties of the bilayer and are hence
108 dependent on the lipid composition. The elastic area expansion modulus reflects the
109 membrane resistance to in plane dilation or stretch [24-26]. The bending modulus is the
110 energy required to bend a membrane from its native curvature to a different curvature
111 [27]. Ever since the first report that amphipaths could potentiate MS channel gating [8],
112 there has been great interest in the effect of bending and local curvature on MS channel
113 function [28-30]. This has been magnified by the determination of the curved structure
114 of Piezo1 channels [31-33].

115
116 Both global properties and lipid-protein interactions are likely to be important for
117 channel function [34-36]. For example, liposomal reconstitution has shown that the
118 bacterial channel MscL is sensitive to bilayer thickness [29, 37, 38], a global property
119 of the bilayer and that the *Mycobacterium tuberculosis* MscL homologue specifically
120 interacts with phosphatidylinositol lipids [20]. In comparison to MscL over the same
121 bilayer thickness range (C16-C20) there is a minor effect on *EcMscS* [38]. We are only
122 beginning to understand the structural basis of how lipids directly interact with *EcMscS*
123 [30, 39-41] particularly as new structures in the presence of lipids become available
124 [42]. Never-the-less previous work suggests this channel may be affected by global
125 changes in bilayer stiffness. This is particularly evident when *EcMscS* is reconstituted
126 into bilayers containing increasing levels of cholesterol, a lipid that increases the elastic
127 area expansion modulus of bilayers [38]. Increasing levels of cholesterol cause the

128 pressure threshold of *EcMscS* to increase. However, many of these studies looking at
129 the sensitivity of *EcMscS* use applied hydrostatic pressure as a surrogate for in plane
130 membrane tension, the parameter that has been shown to correlate most closely with
131 channel activation [43-45]. Furthermore, Piezo1 a eukaryotic mechanosensitive
132 channel that also senses membrane forces has recently been shown to be sensitive to
133 membrane stiffness [46-48].

134

135 Here we investigated how the gating kinetics and tension sensitivity of *EcMscS* were
136 affected by adding defined amounts of lipids with different area expansion moduli to
137 azolectin membranes using patch fluorometry, a technique that combines confocal
138 microscopy and patch clamp electrophysiology [38, 45, 49]. A small amount of a
139 fluorescent lipid such as rhodamine-phosphatidylethanolamine (<0.1% w/w), can be
140 mixed with the desired lipids to accurately follow membrane deformation during patch
141 clamping. This makes it easier to follow membrane deformation which of course can
142 be done in artificial bilayers [50, 51] or cellular systems [52, 53] without the need for
143 fluorescence. By measuring the radius of curvature, the in-plane membrane tension can
144 then be calculated using Laplace's law [54].

145

146 Initially, we aimed to measure the tension sensitivity of purified *EcMscS* in lipid
147 bilayers composed exclusively of dioleoylphosphatidylethanolamine (DOPE) and
148 dioleoylphosphatidylcholine (DOPC). However, none of the combinations of
149 DOPE/DOPC were amenable to the pressure protocol required to accurately measure
150 membrane tension. As a result, we employed azolectin liposomes mixed with lipids of
151 different area expansion modulus. Given that all stiffer lipids caused a significant
152 rightward shift of the *EcMscS* tension response curve, and increased the channel tension
153 threshold, our data clearly implicates membrane stiffness as one of the key determinants
154 of the mechanosensitivity of *EcMscS*.

155

156 **Methods**

157 ***Lipids***

158 This study utilized soybean azolectin from Sigma-Aldrich (P5638). 1,2-dioleoyl-sn-
159 glycerol-3-phosphocholine (DOPC), 1,2-Dioleoyl-sn-glycerol-3-phosphoethanolamine
160 (DOPE), 1,2-diphytanoyl-sn-glycerol-3-phosphocholine (DPhPC), 1,2-diphytanoyl-sn-
161 glycerol-3-phosphoethanolamine (DPhPE), 1,2-distearoyl-sn-glycerol-3-
162 phosphocholine (DSPC), 1,2-Distearoyl-sn-glycerol-3-phosphoethanolamine (DSPE),
163 1,2-dipalmitoleoyl-sn-glycerol-3-phosphoethanolamine (PE 16:1), 1,2-dilinolenoyl-sn-
164 glycerol-3-phosphocholine (PC18:3) and 1,2-dioleoyl-sn-glycerol-3-
165 phosphoethanolamine-N-(lissamine rhodamine B sulfonyl) were purchased from
166 Avanti.

167

168 ***E. coli* MscS protein purification and reconstitution**

169 *E. coli* MscS was purified using a 6xHis-tag according to previously published
170 protocols [55]. Prior to reconstitution the 6xHis-tag was cleaved with thrombin and

171 *EcMscS* was reconstituted into liposomes with different lipid components using the
172 dehydration/rehydration (D/R) reconstitution method. Azolectin was dissolved in
173 chloroform and mixed with the respective lipids of interest. Fluorescent rhodamine-PE
174 is then added at 0.1% before the lipid mixture is dried under nitrogen. The lipid film
175 was then suspended in D/R buffer (200mM KCl, 5mM HEPES, pH adjusted to 7.2 using
176 KOH) and vortexed followed by water bath sonication (6 L 120 W pulse swept power)
177 for 15 minutes. Then 1:50 (w:w) MscS protein was added into the lipid mixture and
178 incubated for 1 hour with agitation, followed by the addition of 300 mg of Biobeads
179 (SM-2, BioRad). The Biobeads were mixed for three hours at room temperature. Finally,
180 the mixture was ultracentrifuged at 40,000 RPM in a Beckman Type 50.2 Ti rotor for
181 30 mins and the lipid mixture was vacuum desiccated overnight. The protein
182 reconstituted liposomes were rehydrated in D/R buffer overnight before use.

183

184 **Electrophysiology**

185 Liposomes were incubated in patch buffer containing: 200mM KCl, 40mM MgCl₂,
186 5mM HEPES adjusted to pH 7.2 using KOH, for one hour until unilamellar blisters
187 formed on their surface. The patch pipette solution and bath solution were
188 symmetric in all recordings containing, in mM: 200 KCl, 40 MgCl₂ and 5
189 HEPES-KOH, pH 7.2. The single channel currents were amplified using an Axopatch
190 200B amplifier (Molecular Devices). The *E. coli* MscS currents were filtered at 2 kHz
191 and sampled at 5 kHz with a Digidata 1440A using pClamp 10 software. Negative
192 hydrostatic pressure was applied in 1s increments by -10 mmHg via a high-speed
193 pressure clamp (ALA Sciences) up to a maximum pressure of -100 mmHg.

194

195 **Patch fluorometry**

196 Wild-type *EcMscS* channels were added to liposomes at a protein:lipid ratio of 1:50
197 (w/w) and recorded by imaging the tip of the patch pipette using a confocal microscope
198 (LSM 700; Carl Zeiss) housed within a Faraday cage and equipped with a water
199 immersion objective lens ($\times 63$, NA1.15). The excised liposome patches that consisted
200 of 99.9% lipids of interest and 0.1% lissamine rhodamine-phosphatidylethanolamine
201 (PE) (w/w) were excited with a 555 nm laser. Fluorescence images of the deformed
202 membranes were acquired and analyzed with ZEN software (Carl Zeiss GmbH). To
203 improve visualization of liposome patches even further the pipette tip was bent
204 approximately 30° with a microforge (MF-900; Narishige, Tokyo, Japan) to make it
205 parallel to the bottom face of the recording chamber. The diameter of the patch dome
206 at each step of pressure was measured using the ZEN software. Tension is calculated
207 using Laplace's law as previously described [45, 49, 54].

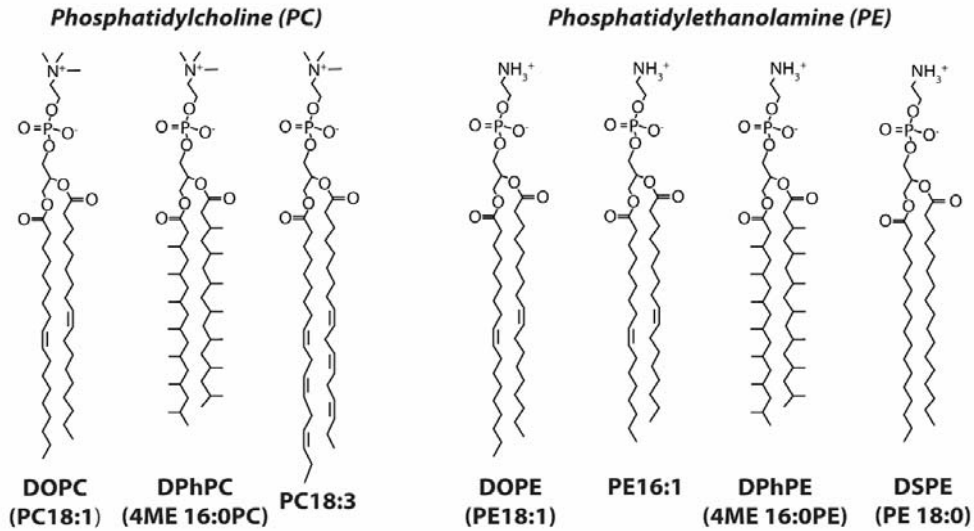
208

209 **Results and discussion**

210 **Sensitivity of *E. coli* MscS in pure DOPC/DOPE bilayers**

211 We first attempted to accurately measure the tension sensitivity of *E. coli* MscS
212 (*EcMscS*) in bilayers exclusively comprised of DOPC (PC18:1) and DOPE (PE18:1).
213 This is due to the fact that previous work shows that membranes composed of PE are
214 stiffer than those of PC [56] and that the rigidity of PC membranes can be increased by

215 the sequential addition of PE [57]. All the lipid types and their corresponding structures
 216 used in this study are shown in Figure 1.
 217



218
 219 **Figure 1. Chemical structure of the lipids used to reconstitute *EcMscS* in this study.**
 220

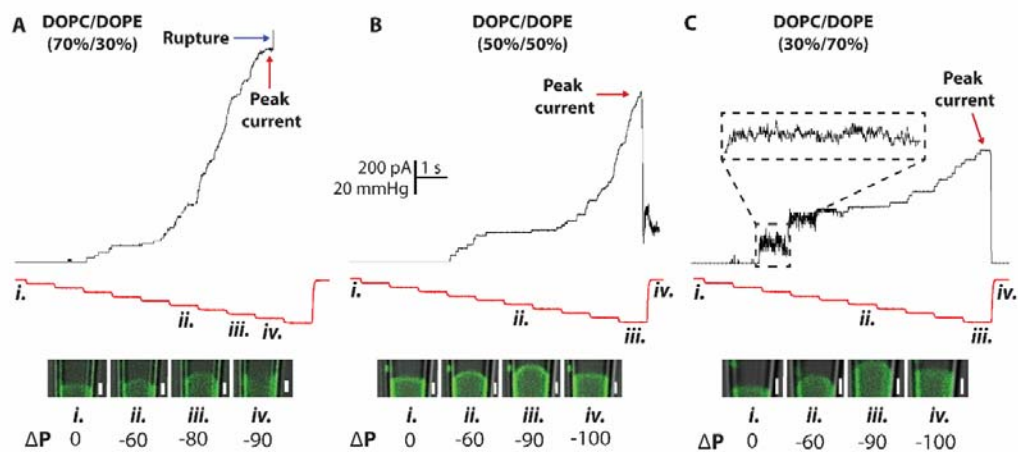
221 In order to accurately measure the tension required to gate *EcMscS* in bilayers, we need
 222 to perform concomitant patch-clamp electrophysiology and confocal microscopy, a
 223 technique referred to as patch fluorometry (Fig. 2A-C). Deformation of the membrane
 224 in response to negative pressure was monitored using a fluorescently labelled lipid that
 225 delineates the membrane, in this case 0.1% rhodamine-PE (Fig. 2A, lower panel). This
 226 was achieved by the application of negative pressure to the pipette tip via a high-speed
 227 pressure clamp. As the pressure was increased the patch dome expanded, stretching the
 228 membrane (Fig. 2A, lower panel i-iv). Laplace's law could then be used to estimate the
 229 tension required to open the channel using the curvature of the patch of membrane.
 230 However, we found that the long stepwise pressure ($1 \text{ s} \times 10 \text{ steps}$) application via a
 231 high-speed pressure clamp necessary to accurately measure the membrane curvature
 232 and ensure equilibration of the membrane was not compatible with pure DOPC/DOPE
 233 bilayers (Fig. 2A-C).
 234

Lipid Composition	Group1: Peak current not reached (patch not ruptured)	Group2: Patch ruptured before peak current	Group3: Peak current reached	Total independent trials
DOPC 100%	N/A	20	N/A	20
DOPC/DOPE 70/30	3	12	1	16
DOPC/DOPE 50/50	7	5	0	12
DOPC/DOPE 30/70	11	2	0	13

235 **Table 1. Statistics associated with individual independent patch fluorometry**
 236 **experiments using pure DOPC and DOPE liposomal membranes.** The table
 237 categorizes each individual patch into three separate groups (Group 1-3). This includes
 238 Group 1: the number of patches where *EcMscS* channel activity did not reach a plateau
 239 despite the application of -100 mmHg but where the patch did not break, Group 2: the
 240 number of patches that ruptured before all channels were activated i.e. a plateau was
 241 not reached, and Group 3: the number of patches where the maximal number of *EcMscS*
 242 channels in the patch were activated and a plateau was reached. The final column
 243 documents the total number of independent patches per lipid group.

244

245 The details of the replicates from DOPC/DOPE bilayers are shown in Table.1 and
 246 representative traces from the most common activity seen is shown in Figure 2. When
 247 *EcMscS* was reconstituted into DOPC/DOPE (70%/30%) liposomes, all channels in the
 248 patch could be activated but this only occurred in 1 out of 16 patches with 12/16 not
 249 surviving the full pressure step protocol (Fig.2A, Table.1). When the concentration of
 250 DOPE was increased the ‘survival rate’ of membrane patches under the pressure
 251 protocol [1s steps in increments of -10 mmHg with a total of 10 steps] was higher
 252 (Table.1). However, in both DOPC/DOPE (50%/50%) and DOPC/DOPE (30%/70%),
 253 the saturation point (peak current) of all *EcMscS* in the patch could not be reached prior
 254 to the membrane reaching its physical limit. Thus, we could not reach peak current of
 255 *EcMscS* and consequently could not accurately measure the tension sensitivity of
 256 *EcMscS* in these membranes. However, we did notice that the gating of *EcMscS* was
 257 more ‘flickery’ in 70%/30% as previously reported (Fig.2C)[18]. We also attempted
 258 patch clamp experiments with *EcMscS* reconstituted into DOPC (100%) but in all
 259 attempts membranes broke before pressure was applied (0/20). We were unable to form
 260 unilamellar blisters in DOPE only (100%).



261

262 **Figure 2. *EcMscS* gating in pure DOPC/DOPE liposomal membranes with**
 263 **corresponding confocal microscopy of the patch dome. (A) Representative patch**
 264 **clamp recording of *EcMscS* reconstituted in DOPC/DOPE (70%/30%) showing that a**
 265 **plateau in peak current does not occur. In this particular example we also see rupture**
 266 **before -100 mmHg is reached (Marked with a blue arrow). (B) Representative patch**

267 clamp recordings of *EcMscS* reconstituted in DOPC/DOPE (50%/50%) showing that a
 268 plateau in peak current does not occur. (C) Representative patch clamp recording of
 269 *EcMscS* reconstituted in DOPC/DOPE (30%/70%), inset shows increased gating
 270 events in this lipid mixture. Black trace represents current and negative pressure steps
 271 applied via high speed pressure clamp are shown in red. Images below represent single
 272 frame images of the membrane (labelled green with 0.1% rhodamine-PE) of the
 273 associated patch-clamp experiment shown above. Each image labelled (i) to (iv)
 274 corresponds to a pressure step labelled on the pressure pulse (coloured red). As the
 275 negative pressure increased from no pressure (i) to a maximum of -100 mmHg the patch
 276 dome expanded. In the case of (A) the final image (iv) shows that the patch had ruptured
 277 and no longer had a clearly defined patch dome. The negative pressure for each image
 278 in mmHg is shown for clarity. Replicates of independent patch experiments associated
 279 with DOPC/DOPE liposomes are shown in Table 1. Inset white bar on images
 280 represents 1 μm .

281

282

283 **The effect of DOPE on *E. coli* MscS threshold.**

284 In order to overcome the issues associated with our pressure protocol (i.e. patch rupture
 285 or channel cohort not reaching maximal activation) and the fragility of DOPC/DOPE
 286 membranes we decided to use azolectin liposomes doped with lipids of interest and
 287 consequently tested the tension sensitivity of *EcMscS*. We chose azolectin as it has been
 288 widely used to reconstitute eukaryotic and prokaryotic ion channels [13, 38, 49, 58].
 289 Azolectin is a lipid mixture primarily composed of PC and as previously mentioned the
 290 sequential addition of PE stiffens PC membranes [57]. Given that PE is the major
 291 constituent of *E. coli* membranes and DOPE is inherently stiffer than DOPC [56] we
 292 first looked at the effect of increasing amounts of DOPE on *EcMscS* gating in azolectin
 293 liposomes. Firstly, our results show that when the concentration of DOPE is above 30%
 294 in the Azolectin (Azo)/DOPE mixture, the gating of *EcMscS* became ‘flickery’.
 295 Flickering was observed in Azo/DOPE (40%/60%) and Azo/DOPE (70%/30%) groups
 296 before the peak current was reached (Fig. 4C & 4A). This increase in the number of
 297 gating events has been documented and quantified previously [18].

298

299

300

Lipid Composition	Number of independent patches	Number of Channels	Open probability Slope [-mN/m] ⁻¹	Midpoint Tension Threshold (MT) (mN/m)
Azo 100%	10	46 ± 7	0.59 ± 0.08	4.4 ± 0.2
Azo/DOPE 90/10	11	89 ± 17	0.58 ± 0.09	4.8 ± 0.4
Azo/DOPE 70/30	11	42 ± 6	0.79 ± 0.10	5.3 ± 0.2
Azo/DOPE 40/60	8	46 ± 8	0.70 ± 0.11	6.7 ± 0.4
Azo/PE 16:1 70/30	7	83 ± 31	0.42 ± 0.04	4.6 ± 0.5

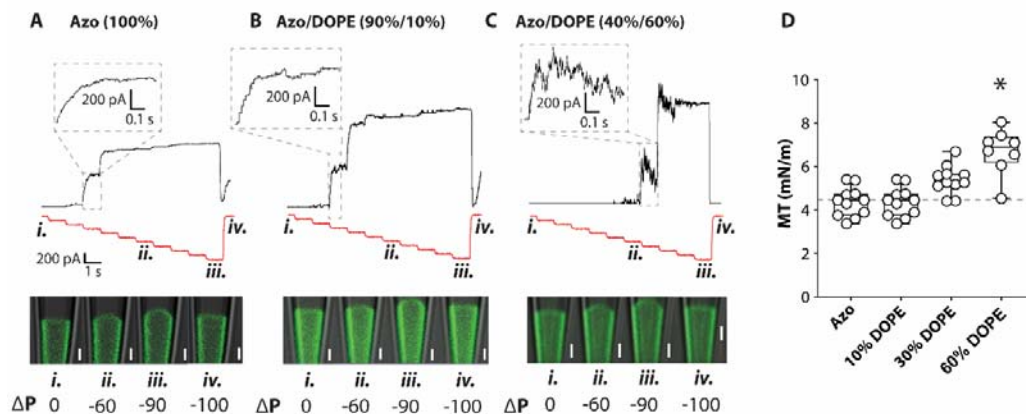
Azo/DPhPE 40/60	5	44 ± 19	0.69 ± 0.17	6.1 ± 0.3
Azo/DSPE 70/30	5	59 ± 16	0.36 ± 0.04	6.3 ± 0.2
Azo/DOPC 70/30	9	17 ± 5	0.67 ± 0.13	2.4 ± 0.2
Azo/PC18:3 70/30	5	32 ± 12	0.48 ± 0.16	2.6 ± 0.2
Azo/DSPC 70/30	10	0 ± 0	ND	ND
Azo/DPhPC 70/30	6	38 ± 9	0.69 ± 0.17	4.8 ± 0.4

301

302 **Table 2.** Channel number, slope and midpoint tension threshold (membrane tension at
 303 which 50% of channels are open) in all azolectin lipid compositions tested in this study.
 304 Data represents mean ± SEM.

305

306 From the activation curve of *EcMscS*, when the concentration of DOPE in the
 307 Azo/DOPE mixture increased, the midpoint tension also increased (Fig.3A-D). The
 308 midpoint tension of *EcMscS* reconstituted into Azolectin (100%) was 4.4 ± 0.2 mN/m
 309 while the threshold in Azo/DOPE (90%/10%), Azo/DOPE (70%/30%), Azo/DOPE
 310 (40%/60%) was 4.8 ± 0.4 mN/m, 5.3 ± 0.2 mN/m and 6.7 ± 0.4 mN/m, respectively.
 311 These values are similar to previous estimates for the midpoint tension of *EcMscS*[38,
 312 45]. These results were not affected by the channel number, because both the average
 313 channel number in Azolectin (100%), in which the channels required the least tension
 314 to open, and Azo/DOPE(40%/60%), in which the channels required the most tension
 315 to open, were similar (Table 2). Importantly, in all our data sets there is little to no
 316 correlation ($R^2 = 0.14$) between the number of channels incorporated and the midpoint
 317 tension threshold (Fig S1 & Table 2).



318

319 **Figure 3** The effects of increasing concentrations of DOPE on the tension sensitivity
 320 of *EcMscS*. (A) Patch clamp recordings of *EcMscS* with corresponding patch
 321 fluorometry images documenting Azolectin (Azo) bilayer deformation (n=8). Images
 322 below represent single frame images of the membrane (labelled green with 0.1%
 323 rhodamine-PE) of the associated patch-clamp experiment shown above. Each image
 324 labelled (i) to (iv) corresponds to a pressure step labelled on the pressure pulse
 325 (coloured red). The negative pressure for each image in mmHg is shown for clarity. (B)
 326 Patch clamp recordings of *EcMscS* with corresponding patch fluorometry images
 327 documenting Azo/DOPE(90%/10%) bilayer deformation (n=11). (C) Patch clamp
 328 recordings of *EcMscS* with corresponding patch fluorometry images documenting

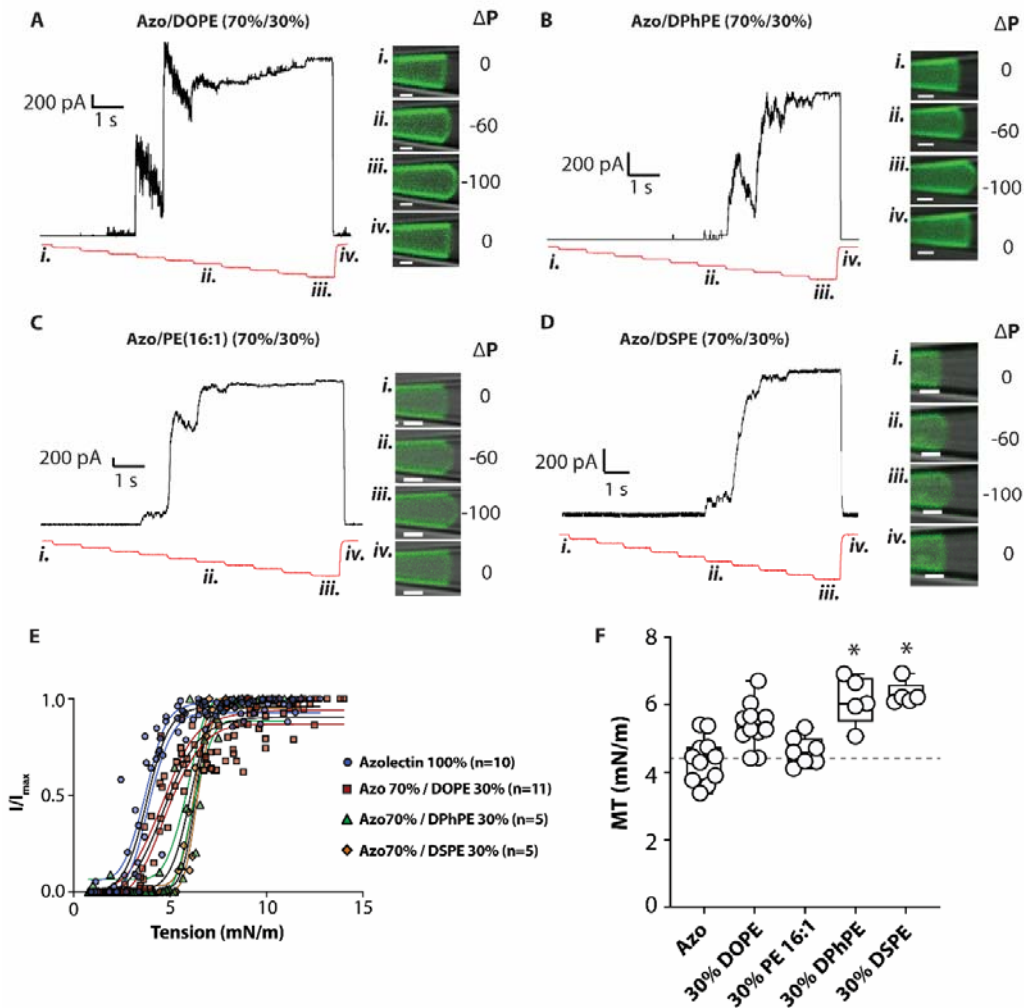
329 *Azo/DOPE(40%/60%) bilayer deformation (n=8). (D) Minimum to maximum box and*
330 *whisker plots showing all data points for the midpoint tension (MT) of EcMscS*
331 *reconstituted in Azolectin, Azo/DOPE(90%/10%), Azo/DOPE(70%/30%) and*
332 *Azo/DOPE(60%/40%). * denotes statistically significant difference from azolectin*
333 *alone using Kruskal-Wallis with Dunn's post hoc test, $p < 0.05$. Inset white bar on*
334 *images represents 1 μ m.*

335

336 **The effect of stiffer forms of PE on *E. coli* MscS tension sensitivity**

337 In order to further interrogate the impact of PE on *EcMscS* tension sensitivity we made
338 use of two forms of PE which are stiffer than DOPE namely DPhPE and DSPE (18:0)
339 (Fig. 4B and D). We found that adding 30% of DPhPE and DSPE to azolectin liposomes
340 caused a significant rightward shift in the tension response curve of *EcMscS* (Fig. 4E,
341 Table 2). The midpoint tension for *EcMscS* in the presence of 30% DPhPE and DSPE
342 were 6.1 ± 0.3 and 6.3 ± 0.2 mN/m, respectively. These rightward shifts were larger in
343 magnitude than measured for DOPE 30% (Fig. 4E, Table 2). DPhPE has a carbon chain
344 length of 16 compared to the c18 of DOPE. In order to ensure that this rightward shift
345 was not due to the different thickness we also tested PE 16:1. Previous work suggests
346 that MscL is sensitive membrane thickness [37] but *EcMscS* is not [38]. As expected
347 PE16:1 did not cause the same significant rightward shift in tension sensitivity as
348 DPhPE (Fig. 4C and E, Table2).

349



350

351 **Figure 4** *The effect of DOPE, DPhPE, PE(16:1), and DSPE on the tension sensitivity*
 352 *of EcMscS. (A) Patch clamp recordings of EcMscS with corresponding patch*
 353 *fluorometry images documenting Azolectin/DOPE (PE18:1) (70%/30%) bilayer*
 354 *deformation (n=11). Images to the right represent single frame images of the membrane*
 355 *(labelled green with 0.1% rhodamine-PE) of the associated patch-clamp experiment.*
 356 *Each image labelled (i) to (iv) corresponds to a pressure step labelled on the pressure*
 357 *pulse (coloured red). The negative pressure for each image in mmHg is shown for*
 358 *clarity. (B) Patch clamp recordings of EcMscS with corresponding patch*
 359 *fluorometry images documenting Azolectin/DPhPE (70%/30%) bilayer deformation*
 360 *(n=5). (C) Patch clamp recordings of EcMscS with corresponding patch fluorometry*
 361 *images documenting Azolectin/PE (PE16:1) (70%/30%) bilayer deformation (n=7). (D)*
 362 *Patch clamp recordings of EcMscS with corresponding patch fluorometry images*
 363 *documenting Azolectin/DSPE (PE18:0) (70%/30%) bilayer deformation (n=5). (E)*
 364 *Tension response curves of EcMscS in all groups compared to azolectin alone shown in*
 365 *blue. Coloured lines represent the 95% confidence intervals for the Boltzmann fits*
 366 *shown in black. (F) Minimum to maximum box and whisker plots showing all data*
 367 *points for the midpoint tension threshold (MT) of EcMscS in each lipid group. * denotes*

368 statistically significant difference from azolectin alone using Kruskal-Wallis with
369 Dunn's post hoc test $p < 0.05$. Inset white bar on images represents $1 \mu\text{m}$.

370

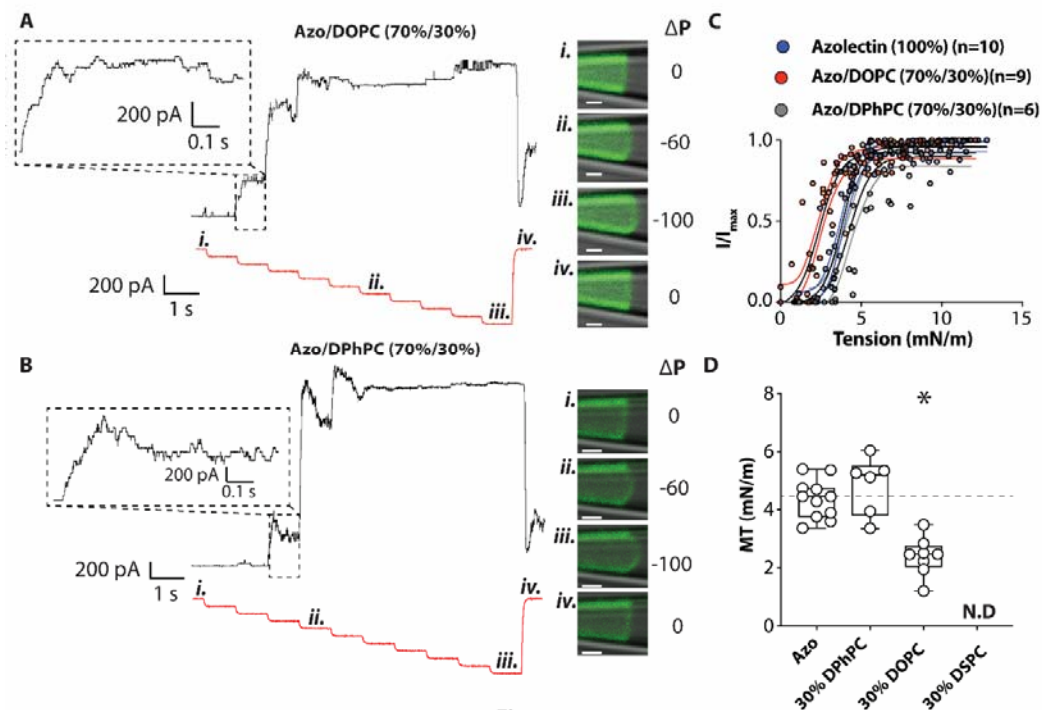
371 The channel flickering also occurred when *EcMscS* was reconstituted in Azo/DPhPE
372 (70%/30%) (Fig.4B) but not in Azo/DSPE (70%/30%). This suggests that different
373 membrane parameters drive the tension sensitivity changes and the kinetic changes.

374

375 The effect of increasing PC content on *E. coli* MscS threshold.

376 We also undertook analogous experiments using PC. *E. coli* MscS reconstituted into
377 Azo/DOPC (70%/30%) liposomes had a higher sensitivity than in Azolectin alone. The
378 midpoint threshold of *EcMscS* in Azo/DOPC (70%/30%) liposomes was 2.4 ± 0.2
379 mN/m which is lower than the midpoint threshold of *EcMscS* in Azolectin (Fig. 5A,
380 Table 2).

381 The channel number in Azo/DOPC (70%/30%) liposomes was much lower than in
382 almost all other groups tested with one exception. In the case of Azo/DSPC (70%/30%)
383 from 10 patches from three separate reconstitutions we could not identify any *EcMscS*
384 activity.



385

386 **Figure 5** The effect of PC on the tension sensitivity of *EcMscS*. (A) Patch clamp
387 recordings of *EcMscS* with corresponding patch fluorometry images documenting
388 Azolectin/DOPC (PC18:1) (70%/30%) bilayer deformation (n=8). (B) Patch clamp
389 recordings of *EcMscS* with corresponding patch fluorometry images documenting
390 Azolectin/DPhPC (70%/30%) bilayer deformation (n=5). (C) Tension response curves
391 of *EcMscS* in all groups compared to azolectin alone are shown in blue. Coloured lines
392 represent 95% confidence intervals for the Boltzmann fits shown in black. (D) Minimum
393 to maximum box and whisker plots showing all data points for the midpoint tension

394 threshold (MT) of *EcMscS* in Azolectin, Azo/DOPC (70%/30%), Azo/DPhPC
 395 (70%/30%) and Azo/DSPC (70%/30%). ND means not determined. * denotes
 396 statistically significant difference from azolectin alone using Kruskal-Wallis with
 397 Dunn's post hoc test, $p < 0.05$. Inset white bar on images represents 1 μm .

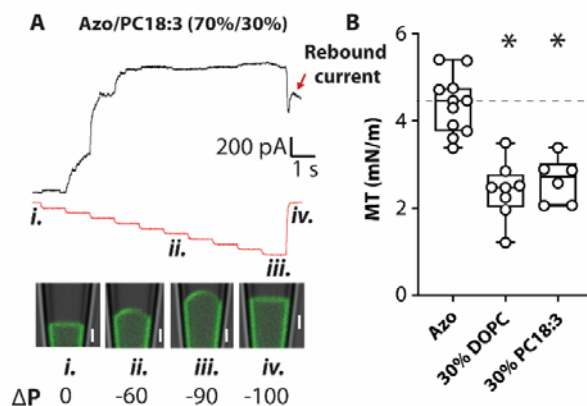
398

399 We compared the tension sensitivity of *EcMscS* in 30% DPhPC to 30% DOPC and a
 400 clear rightward shift was observed (Fig. 5A-C). The midpoint tension of 30% DPhPC
 401 and DPhPE were 4.8 ± 0.4 mN/m (Fig. 5D) and 6.1 ± 0.3 mN/m, respectively (Fig. 4F).
 402 This matches the higher elastic modulus of DPhPE (160 mN/m) when compared to
 403 DPhPC (125 mN/m)[59]. Thus, all our data is congruent with the idea that stiffer
 404 membranes reduce the tension sensitivity of *EcMscS*.

405

406 ***EcMscS* tension sensitivity does not correlate with bending modulus**

407 In all of the cases tested the tension sensitivity of *EcMscS* correlates with both the area
 408 expansion moduli of the lipids (higher the area expansion moduli the higher the tension
 409 required for channel opening) and the bending modulus (higher the bending rigidity the
 410 higher the tension required for channel opening). In order to see which physical
 411 parameter is more important we made use of polyunsaturated acyl chains. In particular
 412 we looked at azolectin liposomes doped with PC18:1 (DOPC) and PC18:3 (Fig 6). The
 413 area expansion moduli of these lipids are almost identical when measured *in vitro* but
 414 the bending rigidity of PC18:3 is half that of PC18:1[60]. We find that the midpoint
 415 tension threshold of *EcMscS* in Azo/PC18:3 (70%/30%) is very similar to that of
 416 azo/PC18:1 (70%/30%) (Fig 6B). This provides further evidence that area expansion
 417 modulus and not bending rigidity is the key determinant of *EcMscS* activity.



418

419 **Figure 6** The effect of PC18:3 on the tension sensitivity of *EcMscS*. (A) Patch clamp
 420 recordings of *EcMscS* with corresponding patch fluorometry images documenting
 421 Azolectin/PC18:3 (70%/30%) bilayer deformation ($n=8$). (B) Minimum to maximum
 422 box and whisker plots showing all data points for the midpoint tension threshold (MT)
 423 of *EcMscS* in Azolectin, Azo/DOPC(70%/30%), Azo/PC18:3(70%/30%). * denotes
 424 statistically significant difference from azolectin alone using Kruskal-Wallis with
 425 Dunn's post hoc test, $p < 0.05$. Inset white bar on images represents 1 μm .

426

427 Here we note that much like Azo/DOPC(70%/30%) and azolectin 100% that *EcMscS*

428 in Azo/PC18:3(70%/30%) shows little to no signs of adaptive behavior i.e. a decline in
 429 current amplitude at constant tension. Patch geometry and mechanics play an important
 430 role in dictating the response of MS channels in patch clamp experiments [61]. From
 431 the confocal microscopy videos of these types of patches, there is no obvious change in
 432 patch geometry that could explain this behavior. This may suggest that there are lipid-
 433 dependent changes in adaptive behavior, which is interesting and warrants further study.
 434 We have previously reported that *EcMscS* reconstituted into azolectin [45, 58] does not
 435 show adaptive gating similar to that seen in *E. coli* spheroplasts [62-65]. Interestingly,
 436 we begin to see signs of adaptive gating in certain lipid types i.e Azolectin doped with
 437 30% DPhPE or DPhPC. Future work should try to decipher whether this is an effect on
 438 adaptation or channel inactivation. It is important here to note that one of the stiffest
 439 lipids the fully saturated lipid DSPE does not show adaptive behavior providing
 440 additional support that our conclusions are still valid even in the presence of adaptive
 441 gating. Moreover, we see broadly similar changes to sensitivity when looking at the
 442 first full channel opening (Fig S2) again further supporting the idea that lipids with a
 443 higher elastic modulus increase the tension required to open the channel.

444 **Rebound activity of *EcMscS* after removal of mechanical stimuli**

445 We noted that on many occasions after the removal of pressure there was a rebound
 446 reactivation of *EcMscS* channels. Figures 7A-B show examples of this rebound activity.
 447 We sought to quantitate whether this rebound activity was more or less common in
 448 certain lipid groups and found that the highest levels of rebound activation were in
 449 liposomes composed of PC lipids. As the levels of PE, particularly stiffer PE types such
 450 as DSPE (PE18:0), increased we saw almost no rebound activation of MscS (Fig. 7C).
 451

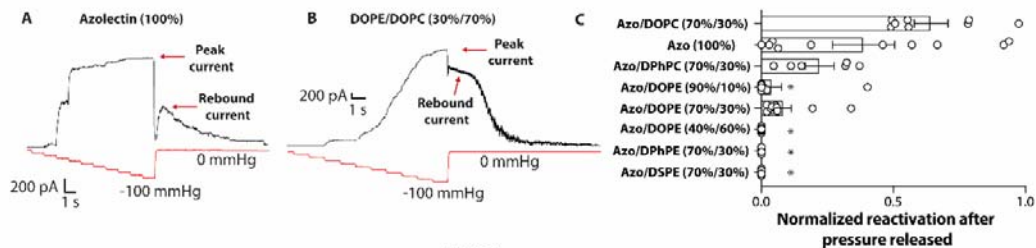


Figure 5

452

453 **Figure 7. Rebound *EcMscS* activity after pressure removal.** (A) Example trace of
 454 *EcMscS* activity reconstituted in Azolectin (100%). Red arrow illustrates the rebound
 455 activity where the negative pressure has been released and returns to 0 mmHg. (B) The
 456 only current trace of *EcMscS* activity reconstituted in DOPE/DOPC (30%/70%) that
 457 progressed through the full negative pressure protocol. Note the exceedingly large
 458 rebound current. (C) Quantitation of the rebound *EcMscS* current by normalizing to the
 459 peak current. Data represents mean \pm SEM ($n = 5-11$), individual data points are shown
 460 for transparency. *denotes statistically significant difference from azolectin alone using
 461 Kruskal-Wallis with Dunn's post hoc test, $p < 0.05$.

462

463 This rebound activation seems to correlate well with the midpoint tension thresholds
 464 suggesting that the rebound activation increases as the membranes become softer (Fig.

465 7C). The phenomenon of ‘rebound’ is typical of shock absorbers, which suppress excess
466 force or rapid movement in mechanical systems. Thus, the rebound MscS activity can
467 be described in this way because the lipid bilayer is elastic, but incorporation of protein
468 may introduce viscoelastic properties. The rapid release of pressure/tension (shock) in
469 the liposome bilayer requires the energy accumulated in the now viscoelastic membrane
470 to be dissipated in some way. In the *EcMscS* case in liposomes this apparently happens
471 through rebound channel activity. The stretching energy stored in the bilayer spring
472 cannot be sufficiently quickly dissipated through the dashpot, which plays a bigger role
473 in soft membranes meaning the softer the membrane the slower becomes the energy
474 dissipation upon sudden release of pressure. Therefore, the rebound effect is larger in
475 softer membranes. This may have implications for *E. coli* osmoregulation and in part
476 explain why their membranes are largely composed of PE. The rapid swelling that
477 occurs in *E. coli* cells as a result of an osmotic downshock is followed by the activation
478 of MS channels that dissipate the generated membrane tension [66]. If the membranes
479 were softer like azolectin or other PC groups, this would result in a rebound activation
480 of the channels and excessive loss of internal solutes. Thus along with the inactivation
481 of the *EcMscS* channel [67] the PE containing membrane may limit excessive
482 activation, maximizing the chance of survival.

483

484 Here, we have avoided the use of lipids with a net charge as these lipids may play a
485 more prominent role in salt bridges that underlie tight protein-lipid interactions with
486 *EcMscS* (i.e R46 [39] or R88[42]). Here we cannot completely rule out the role of direct
487 protein-lipid interactions since PE and PC are zwitterionic lipids and may form
488 electrostatic interaction with MS channels. However, our data suggests that the stiffness
489 of the membrane, in particular the elastic area expansion modulus, is one of the key
490 determinants of *EcMscS* mechanosensitivity. Future work should aim to address the
491 contribution of global effects on bilayer mechanics and direct protein-lipid interactions
492 in *EcMscS* mechanosensitivity.

493

494 **Conclusion**

495 Since the major component in Azolectin is PC which forms membranes with a lower
496 Young’s modulus than membranes formed by PE [56, 57], our results suggest that the
497 stiffer membranes make it harder to open *EcMscS*. Thus, as the PE content becomes
498 larger, we see a rightward shift in the tension response curve of *EcMscS* channel activity.
499 This pattern is retained when comparing either DOPE with DPhPE or DOPC with
500 DPhPC both of which are much stiffer branched lipids. In fact we also know that DPhPE
501 is much stiffer than DPhPC [59] and again we can see that the 30% DPhPE group has
502 a higher midpoint tension threshold than the 30% DPhPC group. This is highly unlikely
503 to be a chain length effect as our work in addition to previous work has conclusively
504 shown that chain length does not markedly affect *EcMscS* tension sensitivity, as it does
505 for *EcMscL* [38]. However, when the same amount of azolectin lipid was replaced by
506 lipids which can form softer membranes, the midpoint tension of *E. coli* MscS becomes
507 lower. For example, when the same amount of azolectin was replaced by DOPC, the
508 channel becomes easier to open. This is the same for PC18:1 and 18:3 providing clear

509 evidence that the critical factor is not bending rigidity. The fact that lipid components
510 can modify the sensitivity of MS channels is key to the activity of the plasma membrane
511 as a mechanochemical transducer [68]. In conclusion, our results strongly suggest that
512 membrane stiffness is one of the key determinants of the mechanosensitivity of *E. coli*
513 MscS channels.

514

515 **Author Contributions**

516 The manuscript was written through contributions of all authors. All authors have given
517 approval to the final version of the manuscript.

518

519 **Funding sources**

520 CDC is supported by a New South Wales Health EMC fellowship, NB is a Chicago
521 Fellow and BM is supported by a Principal Research Fellowship of the National Health
522 and Medical Research Council of Australia. This work was also supported in part by
523 funds from the Office of Health and Medical Research, NSW State Government,
524 Australia.

525

526

527 **References**

528 [1] C.D. Cox, N. Bavi, B. Martinac, Bacterial Mechanosensors, Annual review of
529 physiology 80(1) (2018) null.

530 [2] J.H. Naismith, I.R. Booth, Bacterial mechanosensitive channels--MscS: evolution's
531 solution to creating sensitivity in function, Annual review of biophysics 41 (2012)
532 157-77.

533 [3] N. Levina, S. Totemeyer, N.R. Stokes, P. Louis, M.A. Jones, I.R. Booth, Protection
534 of *Escherichia coli* cells against extreme turgor by activation of MscS and MscL
535 mechanosensitive channels: identification of genes required for MscS activity, EMBO
536 J 18(7) (1999) 1730-7.

537 [4] C.D. Cox, Y. Nakayama, T. Nomura, B. Martinac, The evolutionary 'tinkering' of
538 MscS-like channels: generation of structural and functional diversity, Pflugers Arch
539 (2015).

540 [5] E.S. Hamilton, A.M. Schlegel, E.S. Haswell, United in diversity: mechanosensitive
541 ion channels in plants, Annual review of plant biology 66 (2015) 113-37.

542 [6] T. Rasmussen, A. Rasmussen, Bacterial Mechanosensitive Channels, Subcell Biochem
543 87 (2018) 83-116.

544 [7] J. Teng, S. Loukin, A. Anishkin, C. Kung, The force-from-lipid (FFL) principle
545 of mechanosensitivity, at large and in elements, Pflugers Arch (2015).

546 [8] B. Martinac, J. Adler, C. Kung, Mechanosensitive ion channels of *E. coli* activated
547 by amphipaths, Nature 348(6298) (1990) 261-3.

548 [9] S. Sukharev, Purification of the small mechanosensitive channel of *Escherichia*
549 *coli* (MscS): the subunit structure, conduction, and gating characteristics in
550 liposomes, Biophysical journal 83(1) (2002) 290-8.

551 [10] E. Petrov, D. Palanivelu, M. Constantine, P.R. Rohde, C.D. Cox, T. Nomura, D.L.
552 Minor, Jr., B. Martinac, Patch-clamp characterization of the MscS-like

553 mechanosensitive channel from *Silicibacter pomeroyi*, *Biophys J* 104(7) (2013) 1426–
554 34.

555 [11] C.D. Cox, C. Bae, L. Ziegler, S. Hartley, V. Nikolova-Krstevski, P.R. Rohde,
556 C.A. Ng, F. Sachs, P.A. Gottlieb, B. Martinac, Removal of the mechanoprotective
557 influence of the cytoskeleton reveals PIEZO1 is gated by bilayer tension, *Nature*
558 *communications* 7 (2016) 10366.

559 [12] R. Syeda, Maria N. Florendo, Charles D. Cox, J.M. Kefauver, Jose S. Santos,
560 B. Martinac, A. Patapoutian, Piezo1 Channels Are Inherently Mechanosensitive, *Cell*
561 *reports* 17(7) (2016) 1739–1746.

562 [13] S.G. Brohawn, Z. Su, R. MacKinnon, Mechanosensitivity is mediated directly by
563 the lipid membrane in TRAAK and TREK1 K⁺ channels, *Proceedings of the National*
564 *Academy of Sciences of the United States of America* 111(9) (2014) 3614–9.

565 [14] S.E. Murthy, A.E. Dubin, T. Whitwam, S. Jojoa Cruz, S.M. Cahalan, S.A. Mosavi,
566 A.B. Ward, A. Patapoutian, OSCA/TMEM63 are an evolutionarily conserved family of
567 mechanically activated ion channels, *eLife* 7 (2018).

568 [15] C.D. Cox, N. Bavi, B. Martinac, Origin of the Force: The Force-From-Lipids
569 Principle Applied to Piezo Channels, *Current Topics in Membranes*, Academic Press 2016.

570 [16] C.D. Cox, N. Bavi, B. Martinac, Biophysical Principles of Ion-Channel-Mediated
571 Mechanosensory Transduction, *Cell reports* 29(1) (2019) 1–12.

572 [17] S. Sukharev, F. Sachs, Molecular force transduction by ion channels: diversity
573 and unifying principles, *J Cell Sci* 125(Pt 13) (2012) 3075–83.

574 [18] P. Ridone, Y. Nakayama, B. Martinac, A.R. Battle, Patch clamp characterization
575 of the effect of cardiolipin on MscS of *E. coli*, *Eur Biophys J* 44(7) (2015) 567–76.

576 [19] P. Ridone, S.L. Grage, A. Patkunarajah, A.R. Battle, A.S. Ulrich, B. Martinac,
577 “Force-from-lipids” gating of mechanosensitive channels modulated by PUFAs, *J Mech*
578 *Behav Biomed Mater* 79 (2018) 158–167.

579 [20] D. Zhong, P. Blount, Phosphatidylinositol is crucial for the mechanosensitivity
580 of *Mycobacterium tuberculosis* MscL, *Biochemistry* 52(32) (2013) 5415–20.

581 [21] D. Zhong, L.M. Yang, P. Blount, Dynamics of protein-protein interactions at the
582 MscL periplasmic-lipid interface, *Biophysical journal* 106(2) (2014) 375–81.

583 [22] J.F. Cordero-Morales, V. Vasquez, How lipids contribute to ion channel function,
584 a fat perspective on direct and indirect interactions, *Current opinion in structural*
585 *biology* 51 (2018) 92–98.

586 [23] R.S. Cantor, The lateral pressure profile in membranes: a physical mechanism of
587 general anesthesia, *Toxicol Lett* 100–101 (1998) 451–8.

588 [24] E. Evans, W. Rawicz, B.A. Smith, Back to the future: mechanics and thermodynamics
589 of lipid biomembranes, *Faraday Discuss* 161 (2013) 591–611.

590 [25] D. Needham, R.S. Nunn, Elastic deformation and failure of lipid bilayer membranes
591 containing cholesterol, *Biophys J* 58(4) (1990) 997–1009.

592 [26] W. Rawicz, B.A. Smith, T.J. McIntosh, S.A. Simon, E. Evans, Elasticity, strength,
593 and water permeability of bilayers that contain raft microdomain-forming lipids,
594 *Biophys J* 94(12) (2008) 4725–36.

595 [27] J.F. Nagle, M.S. Jablin, S. Tristram-Nagle, K. Akabori, What are the true values
596 of the bending modulus of simple lipid bilayers?, *Chem Phys Lipids* 185 (2015) 3–10.

597 [28] O. Bavi, C.D. Cox, M. Vossoughi, R. Naghdabadi, Y. Jamali, B. Martinac, Influence
598 of Global and Local Membrane Curvature on Mechanosensitive Ion Channels: A Finite
599 Element Approach, *Membranes* 6(1) (2016).

600 [29] E. Perozo, D.M. Cortes, P. Sompornpisut, A. Kloda, B. Martinac, Open channel
601 structure of MscL and the gating mechanism of mechanosensitive channels, *Nature*
602 418(6901) (2002) 942–8.

603 [30] C. Pliotas, A.C. Dahl, T. Rasmussen, K.R. Mahendran, T.K. Smith, P. Marius, J.
604 Gault, T. Banda, A. Rasmussen, S. Miller, C.V. Robinson, H. Bayley, M.S. Sansom, I.R.
605 Booth, J.H. Naismith, The role of lipids in mechanosensation, *Nature structural &*
606 *molecular biology* 22(12) (2015) 991–8.

607 [31] Y.R. Guo, R. MacKinnon, Structure-based membrane dome mechanism for Piezo
608 mechanosensitivity, *eLife* 6 (2017).

609 [32] K. Saotome, S.E. Murthy, J.M. Kefauver, T. Whitwam, A. Patapoutian, A.B. Ward,
610 Structure of the mechanically activated ion channel Piezo1, *Nature* 554(7693) (2018)
611 481–486.

612 [33] Q. Zhao, H. Zhou, S. Chi, Y. Wang, J. Wang, J. Geng, K. Wu, W. Liu, T. Zhang,
613 M.Q. Dong, J. Wang, X. Li, B. Xiao, Structure and mechanogating mechanism of the
614 Piezo1 channel, *Nature* 554(7693) (2018) 487–492.

615 [34] P. Wiggins, R. Phillips, Membrane-protein interactions in mechanosensitive
616 channels, *Biophys J* 88(2) (2005) 880–902.

617 [35] D. Balleza, Mechanical properties of lipid bilayers and regulation of
618 mechanosensitive function: from biological to biomimetic channels, *Channels (Austin)*
619 6(4) (2012) 220–33.

620 [36] K. Yoshimura, M. Sokabe, Mechanosensitivity of ion channels based on protein-
621 lipid interactions, *J R Soc Interface* 7 Suppl 3 (2010) S307–20.

622 [37] E. Perozo, A. Kloda, D.M. Cortes, B. Martinac, Physical principles underlying
623 the transduction of bilayer deformation forces during mechanosensitive channel gating,
624 *Nat Struct Biol* 9(9) (2002) 696–703.

625 [38] T. Nomura, C.G. Cranfield, E. Deplazes, D.M. Owen, A. Macmillan, A.R. Battle,
626 M. Constantine, M. Sokabe, B. Martinac, Differential effects of lipids and lyso-
627 lipids on the mechanosensitivity of the mechanosensitive channels MscL and MscS,
628 *Proceedings of the National Academy of Sciences of the United States of America*
629 109(22) (2012) 8770–5.

630 [39] T. Rasmussen, V.J. Flegler, A. Rasmussen, B. Bottcher, Structure of the
631 Mechanosensitive Channel MscS Embedded in the Membrane Bilayer, *Journal of molecular*
632 *biology* (2019).

633 [40] T. Rasmussen, A. Rasmussen, L. Yang, C. Kaul, S. Black, H. Galbiati, S.J. Conway,
634 S. Miller, P. Blount, I.R. Booth, Interaction of the Mechanosensitive Channel, MscS,
635 with the Membrane Bilayer through Lipid Intercalation into Grooves and Pockets, *J*
636 *Mol Biol* (2019).

637 [41] N. Bavi, C.D. Cox, E. Perozo, B. Martinac, Toward a structural blueprint for
638 bilayer-mediated channel mechanosensitivity, *Channels (Austin)* 11(2) (2017) 91–93.

639 [42] B. Reddy, N. Bavi, A. Lu, Y. Park, E. Perozo, Molecular basis of force-from-
640 lipids gating in the mechanosensitive channel MscS, *Elife* 8 (2019).

641 [43] P. Moe, P. Blount, Assessment of potential stimuli for mechano-dependent gating
642 of MscL: effects of pressure, tension, and lipid headgroups, *Biochemistry* 44(36)
643 (2005) 12239-44.

644 [44] T. Rasmussen, How do mechanosensitive channels sense membrane tension?,
645 *Biochemical Society transactions* 44(4) (2016) 1019-25.

646 [45] T. Nomura, C.D. Cox, N. Bavi, M. Sokabe, B. Martinac, Unidirectional
647 incorporation of a bacterial mechanosensitive channel into liposomal membranes, *FASEB*
648 *J* 29(10) (2015) 4334-45.

649 [46] L.O. Romero, A.E. Massey, A.D. Mata-Daboin, F.J. Sierra-Valdez, S.C. Chauhan,
650 J.F. Cordero-Morales, V. Vasquez, Dietary fatty acids fine-tune Piezo1 mechanical
651 response, *Nature communications* 10(1) (2019) 1200.

652 [47] W. Zheng, Y.A. Nikolaev, E.O. Gracheva, S.N. Bagriantsev, Piezo2 integrates
653 mechanical and thermal cues in vertebrate mechanoreceptors, *Proceedings of the*
654 *National Academy of Sciences* (2019) 201910213.

655 [48] P. Ridone, E. Pandzic, M. Vassalli, C.D. Cox, A. Macmillan, P.A. Gottlieb, B.
656 Martinac, Disruption of membrane cholesterol organization impairs the concerted
657 activity of PIEZO1 channel clusters, (2019) 604488.

658 [49] N. Bavi, Y. Nakayama, O. Bavi, C.D. Cox, Q.H. Qin, B. Martinac, Biophysical
659 implications of lipid bilayer rheometry for mechanosensitive channels, *Proceedings*
660 *of the National Academy of Sciences of the United States of America* 111(38) (2014)
661 13864-9.

662 [50] S.I. Sukharev, W.J. Sigurdson, C. Kung, F. Sachs, Energetic and spatial
663 parameters for gating of the bacterial large conductance mechanosensitive channel,
664 *MscL*, *J Gen Physiol* 113(4) (1999) 525-40.

665 [51] M. Sokabe, F. Sachs, Z.Q. Jing, Quantitative video microscopy of patch clamped
666 membranes stress, strain, capacitance, and stretch channel activation, *Biophys J*
667 59(3) (1991) 722-8.

668 [52] A.H. Lewis, J. Grandl, Mechanical sensitivity of Piezo1 ion channels can be
669 tuned by cellular membrane tension, *Elife* 4 (2015).

670 [53] G. Maksaev, A. Milac, A. Anishkin, H.R. Guy, S. Sukharev, Analyses of gating
671 thermodynamics and effects of deletions in the mechanosensitive channel TREK-1:
672 comparisons with structural models, *Channels (Austin)* 5(1) (2011) 34-42.

673 [54] S. Shaikh, C.D. Cox, T. Nomura, B. Martinac, Energetics of gating MscS by
674 membrane tension in azolectin liposomes and giant spheroplasts, *Channels (Austin)*
675 8(4) (2014) 321-6.

676 [55] V. Vasquez, D.M. Cortes, H. Furukawa, E. Perozo, An optimized purification and
677 reconstitution method for the MscS channel: strategies for spectroscopical analysis,
678 *Biochemistry* 46(23) (2007) 6766-73.

679 [56] K. Katsov, M. Muller, M. Schick, Field theoretic study of bilayer membrane
680 fusion. I. Hemifusion mechanism, *Biophysical journal* 87(5) (2004) 3277-90.

681 [57] R. Dawaliby, C. Trubbia, C. Delporte, C. Noyon, J.M. Ruyschaert, P. Van
682 Antwerpen, C. Govaerts, Phosphatidylethanolamine Is a Key Regulator of Membrane
683 Fluidity in Eukaryotic Cells, *J Biol Chem* 291(7) (2016) 3658-67.

684 [58] C.D. Cox, T. Nomura, C.S. Ziegler, A.K. Campbell, K.T. Wann, B. Martinac,

685 Selectivity mechanism of the mechanosensitive channel MscS revealed by probing
686 channel subconducting states, *Nature communications* 4 (2013) 2137.

687 [59] A. Yasmann, S. Sukharev, Properties of diphytanoyl phospholipids at the air-
688 water interface, *Langmuir* 31(1) (2015) 350-7.

689 [60] W. Rawicz, K.C. Olbrich, T. McIntosh, D. Needham, E. Evans, Effect of chain
690 length and unsaturation on elasticity of lipid bilayers, *Biophysical journal* 79(1)
691 (2000) 328-39.

692 [61] T.M. Suchyna, V.S. Markin, F. Sachs, Biophysics and structure of the patch and
693 the gigaseal, *Biophys J* 97(3) (2009) 738-47.

694 [62] U. Cetiner, A. Anishkin, S. Sukharev, Spatiotemporal relationships defining the
695 adaptive gating of the bacterial mechanosensitive channel MscS, *Eur Biophys J* 47(6)
696 (2018) 663-677.

697 [63] B. Akitake, A. Anishkin, S. Sukharev, The "dashpot" mechanism of stretch-
698 dependent gating in MscS, *J Gen Physiol* 125(2) (2005) 143-54.

699 [64] X. Wang, S. Tang, X. Wen, L. Hong, F. Hong, Y. Li, Transmembrane TM3b of
700 Mechanosensitive Channel MscS Interacts With Cytoplasmic Domain Cyto-Helix, *Front*
701 *Physiol* 9 (2018) 1389.

702 [65] H.R. Malcolm, P. Blount, Mutations in a Conserved Domain of *E. coli* MscS to the
703 Most Conserved Superfamily Residue Leads to Kinetic Changes, *PLoS One* 10(9) (2015)
704 e0136756.

705 [66] I.R. Booth, Bacterial mechanosensitive channels: progress towards an
706 understanding of their roles in cell physiology, *Curr Opin Microbiol* 18 (2014) 16-
707 22.

708 [67] M. Boer, A. Anishkin, S. Sukharev, Adaptive MscS gating in the osmotic
709 permeability response in *E. coli*: the question of time, *Biochemistry* 50(19) (2011)
710 4087-96.

711 [68] A.L. Le Roux, X. Quiroga, N. Walani, M. Arroyo, P. Roca-Cusachs, The plasma
712 membrane as a mechanochemical transducer, *Philos Trans R Soc Lond B Biol Sci* 374(1779)
713 (2019) 20180221.

714